Materials Physics and Mechanics 25 (2016) 22-29 Received: October 15, 2015

STRUCTURAL INTEGRITY OF STEEL BAR UNDER SEISMIC LOADS

Alk. Apostolopoulos[1*], T. Matikas[1], G. Kodzhaspirov[2]

[1]University of Ioannina, P.O. Box 1186, Ioannina, 45110, Greece

[2]Peter the Great St. Petersburg Polytechnic University, Polytechnicheskaya 29, St. Petersburg, 195251, Russia

*e-mail: prosthesis.apostolopoulos@gmail.com

Abstract. In the current study, a research was conducted in three different steel categories of high and medium ductility such as B400c, B450c and B500b under seismic loads which were simulated with low cycle fatigue tests. Based on the results of mechanical tests, SEM and EDX on the above steel specimens before and after accelerated corrosion it is important to mention the negative role of sulfides, as it is mainly MnS inclusions, with existence of chloride ions and buckling phenomena in Structural Integrity of rebars.

1. Introduction

The widespread occurrence of corrosion on rebars in existing reinforced concrete structures is a common problem with many consequences. Especially, the coastal environment with high content of chloride ions as well as the extensive use of chloride salt snow-melting agent in winter exacerbates the effects of the corrosive action on steel reinforcing bars of structures. Seismic loads are known to act on the load bearing elements of structures in the form of high strain reversals, which can be simulated as single axis Low Cycle Fatigue. The Fourier spectra of ground movement during an earthquake which occurred in Japan showed that the loading was cyclic and the frequency corresponding to the maximum amplitude was approximately 2 Hz. Investigation of the catastrophic earthquake of Tang Shan in China confirmed that the failure mode of the building structural steel was LCF [1].

Earthquakes inflict cumulative damage on reinforced concrete structures but most codes do not explicitly take it into account. In current design practice a displacement ductility coefficient is used which however fails to account for the accumulated damage since it is implicitly assumed that structural damage occurs only due to the maximum response deformation and is independent of the number of non-peak inelastic cycles or strain energy dissipation. All inelastic cycles however must be considered as contributors to damage since they constitute the strain history observed in actual structures and their accumulation may become important depending on the characteristics of the ground motion [2]. During strong earthquakes, yielding structures are subjected to increased number of cycles into the inelastic range and the accumulated damage may significantly affects their overall performance. This type of damage may also evolve from multiple earthquakes, in which case, a series of pre or post shocks combined with the main shock may be treated as a single event of extended duration. Assessment of seismic damage is usually assumed to be similar to metal fatigue under a variable amplitude of cyclic loading. Relatively little attention has been devoted by the research community on the combined effect of corrosion and LCF on rebars since each one of these factors affect the rebar durability and performance and shortens the design life of structures [3-9]. In addition, the deficiency of the research is even stronger in high ductility steels which are widely used in the European community and have a dual phase or triple phase structure as B400c, B500b and B450c.

Without a doubt, when critical elements of structures (columns, beams etc.) are under dual adverse effects of chloride ion corrosive environment and strong earthquakes, the steel reinforcement is under coupling effects of corrosion and low cycle fatigue. Under of the above circumstances the performance of RC bridge structures deteriorates rapidly. Therefore, it hasimportant practical significance to carry out research on performance deterioration of corroded RC columns and reinforcing bars under seismic loads.

In the present study an experimental investigation was conducted in order to evaluate the effect of corrosion on B400c, B450c and B500b, 16 mm diameter reinforcing ribbed steel bars. The changes in mass loss and LCF behavior under constant strain amplitude were measured. Mass loss and LCF behavior are critical for the safety and remaining life of corroded structures that are located within seismic zones such as Mediterranean countries (Italy, Greece, Turkey etc.). At the same time are investigated the consequences of the action of chlorides in MnS inclusion in the rebars and their synergy with buckling phenomena in Structural Integrity of Steel bar under seismic loads.

2. Experimental work

2.1. Corrosion induced mass loss. The mechanism of chloride induced corrosion is analyzed and some of its consequences on the performance of different steel bars are experimentally measured and compared each other. The present approach will contribute towards the modeling of the total deterioration cycle, including initiation and propagation periods. It should be emphasized that accelerated salt spray corrosion tests on bare rebars theoretically lead to different results than those that could occur on embedded in concrete rebars. However, the present results represent a good first approximation of the influence of accelerated corrosion on steel ductility properties versus exposure of embedded rebars in a natural corrosive environment. This would require years to reach similar levels of deterioration since concrete delays the chloride penetration depending on its physical and chemical characteristics. When the chlorides reach the reinforcement and exceed a critical concentration level then the corrosion process takes place almost similarly with the case of bare bars.

Ribbed B400c, B500b and B450c steel bars, 16 mm diameter, were sprayed in a salt spray corrosion chamber, according to ASTM B117- 94 specification, for 90 days, with a 5 % sodium chloride and 95 % distilled water solution, pH range of 6.5–7.2, and temperature of 35 +1.1–1.7 °C. Pitting was initiated progressively on the specimens after 10, 20 and 30 days of corrosion which became progressively more severe. Upon completion of the salt spray the specimens were washed carefully with clean water according to ASTM G1-72 procedure in order to remove any leftover salt deposits and then were dried.

The stereoscopic images show the pitting on the steel surfaces which are developed even after removal of the rust. The relatively large pits at 10 days of exposure suggest that these are the active sites at which corrosion is primarily taking place. Pitting appeared to be initiated at the reinforcement veins of the steel bars and proceeded to the intermediate space. In addition cavities and notches were formed on the steel surface and especially in the rib bases, which became progressively more severe as the corrosion level increased. The average pit depth, after 90 days of corrosion, was approximately 0.05 mm with maximum value of 0.45 mm, according to ASTM G 46-94 specification which is the guide for examination and evaluation of pitting corrosion. The specimens along their entire length were covered with natural wax, except a portion of length , at least, 20 mm, to allow for a single rib spacing (distance between two successive ribs) in the middle of each specimen. The testing specimens were placed at an angle of 45-60 degrees in the salt spray chamber (ISO 9227). During the full duration of the experiment, the specimens were replaced every day. Every day was planned to take place 8 wet/dry cycles, which means that 90 minutes dry followed by 90 minutes wet environment. During the experimental procedure a digital measurement of pH was monitoring chamber’s environment.

2.2. Mechanical testing procedure. The steel rebars were produced by European industries and were delivered in the form of ribbed bars. The nominal diameter of the rebars was 16mm (Φ16). From low cycle fatigue specimens a length of 205-210 mm was cut. The free length of the specimen between the grips was set to be six times the nominal diameter Φ16 which means 96 mm length. Prior to the mechanical tests, the specimens were corroded using accelerated laboratory corrosion tests in salt spray environment. The number of specimens taking into account all the previously mentioned parameters are defined as illustrated in Table 1.

Table 1. Number of Samples tested in LCF for each Steel Grade.

	Bar Diameter	Frequency, Hz	Free Length	Imposed Deformation, ε, %	Tests for each Grade		
					0	90	
B450C	16 mm	2,0	6Φ	± 2,5 %	5	3	17
				± 4,0 %	5	4	
B400C			6Φ	± 2,5 %	4	3	14
				± 4,0 %	4	3	
B500B			6Φ	± 2,5 %	4	3	15
				± 4,0 %	4	4	
					26	20	
Total of LCF tests categorized ± 2,5 %				22			
Total of LCF tests categorized ± 4,0 %				24			

The low-cycle fatigue tests aim to provide information on the followings:

a. On the effect of various accelerated salt spray corrosion levels on the dissipated energy density and the number of cycles to failure of each grade steel bars.

b. On the combined effect of corrosion and low cycle fatigue on the load bearing ability of the reinforcing steel.

All mechanical tests were conducted at room temperature using an MTS 250 KN servo-hydraulic testing system. All readings were recorded using a fully automated computer system. A number of low cycle fatigue tests for each corrosion level were conducted for two different strain levels ± 2.5 % and ± 4 %, totaling a number of 46 low cycle fatigue tests.

Table 2 (a, b), from Ref. [10] experimental study, shows the results of mechanical tensile tests of B400c, B450c and B500bsteel rebars. These tests were conducted according to ISO 15630-1 and specimens length was set to 580 mm. The tensile tests were carried out on a servo-hydraulic MTS 250 kN universal testing machine and from the tests the yield stress Rp, tensile strength Rm, elongation to tensile strength Agt and Energy Density U were evaluated.

Table 2 shows the minimum standards for medium and high ductility steel set by the EuroCode 2 (EC2).

Table 2(a). Average value of mechanical properties of pre-corroded specimens.

Steel Class	Yield R_p [MPa]	Elongation A_{gt} [%]	Minimum values $k=[R_p/R_m]_k$
$B500_B$	500	≥5	≥1.08
$B400_C$	400	≥7.5	≥ 1.15 <1.35
$B450_C$	450	≥7.5	≥ 1.15 <1.35

Table 2(b).

Grade	$R_{\rho\theta.2}$, MPa	R_m, MPa	$R_m/R_{\rho\theta.2}$	ε_{100}, %	A_{gt}, %	U, MPa
B400$_C$	435	549.23	1.26	15.33	15.6	78.06
B450$_C$	536.4	647.95	1.21	11.48	11.6	69.75
B500$_B$	523	638.35	1.22	14.03	14.4	82.83

3. The role of MnS inclusion

MnS inclusions play a leading role in the initial corrosion because chloride prefers to be adsorbed and accumulate in MnS inclusions, resulting in pitting corrosion [10-12]. From cross sections tobiphasic steel rebars B400c, B500b and B450c, Φ16, before and after corrosion merged areas with MnS inclusions. The MnS inclusions with the coexistence of other voids and crevice areas represent regions of degradation of the consistency of the material of steel. The Figure 1 shows EDX with chlorideions which have intruded in material’s structure and similar regions where MnS inclusions have been dissolved. The impurities appear to be positioned at a distance between 20 and 500 μm from the surface and well within the martensite zone.

In Ref. [10] experimental study, the mechanical behavior in three types of reinforced concrete steel was examined. An evaluation of the mechanical behavior in dual phase steels B400c, B450c and B500b of high and medium ductility class, with a 16mm nominal diameter, was conducted before and after exposure in laboratory salt spray environment. The results of all mechanical tensile tests were compared and combined with the results of SEM and EDX analysis and consequently led to the following findings: The strength properties reduction in pre-corroded specimens was almost equivalent to the mass loss which meets the demands set by Euro Code 2 (EC2) for safe structures. However, the drop in ductility properties, expressed as the deformation at maximum strength, is below the minimum limits. The findings also suggest that the degradation in the mechanical performance of steel cannot be attributed to a specific mechanism but it appears to be the result of several interrelated factors, such as the development of pits in the outer surface of steel and various side effects within the martensitic layer, which occur from the presence of extensive porosity close to the surface as well as several sulfide compounds, like MnS. Similar findings have been presented in project [14].

The Figs. 2, 3 and 4 show the identification of MnS inside the section of steel rebars, their development and their connection to other external damages due to crevice areas and pit corrosion after 90 days exposure to corrosion. The growth of the degree of damage due to the rapid deterioration of MnS areas endangers the structural integrity of steel rebars because of potential join with other surface pits. The above view about MnS areas is confirmed by E.G. Webb et al. [14] studies. In these studies is expressed the view that the pitting susceptibility of MnS inclusions in chloride containing solutions is attributed to a preferential adsorption of chloride ions at these inclusions, which results in the chemical or electrochemical dissolution of MnS inclusions when the reinforcing steel is at a resting potential.

According to [13, 15] studies the pitting susceptibility of MnS inclusions in chloride containing solutions is attributed to a preferential adsorption of chloride ions at these inclusions, which results in the chemical or electrochemical dissolution of MnS inclusions when the reinforcing steel is at a resting potential. Additionally in [13] and [15] studies is expressed the view that this dissolution is generally accompanied by a local drop in pH around the regions of MnS inclusions. The stable pitting nuclei accelerated the dissolution of Fe, and further hydrolysis reactions of Fe ions continued to reduce the local pH and this accelerates dissolution of the anode. As a result, corrosion of the rebar becomes more severe, while the potential mapping provided a sharp peak on the potential map and the distribution of chloride and S at the corrosion sites. In EDX of Fig. 1 are shown chloride ions appears to be trapped within the region where MnS inclusions have been dissolved, outside these regions in which MnS inclusions are present, Cl – is not observed.

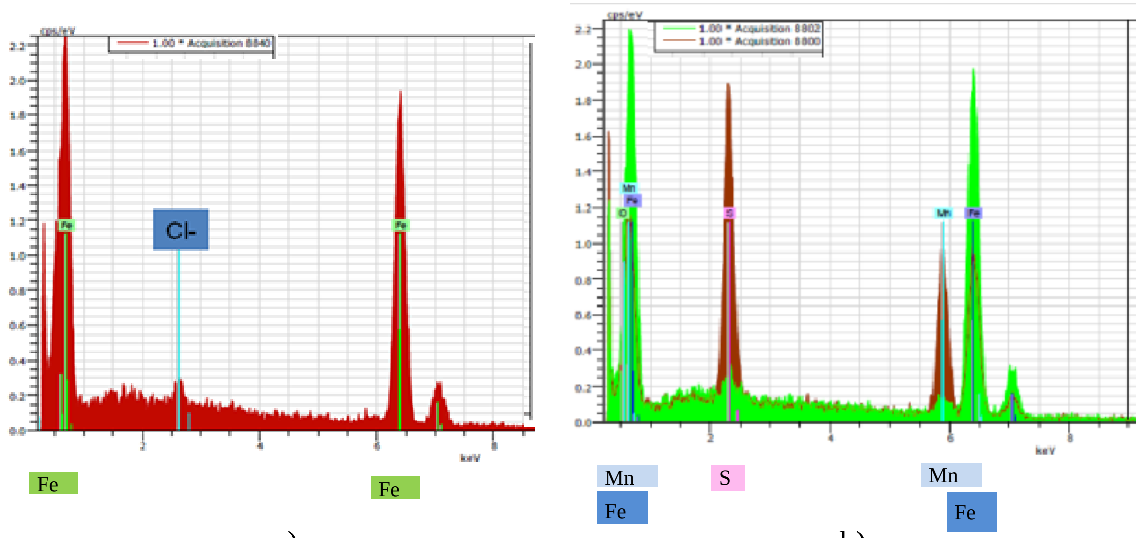

a) b)

Fig. 1. a) chloride ions and b) region where MnS inclusions have been dissolved.

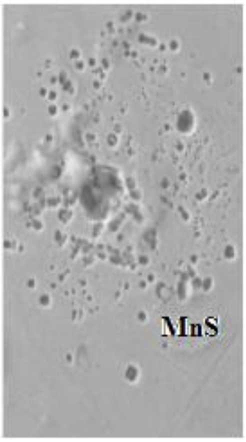

Fig. 2. MnS areas on cross section of steel rebar.

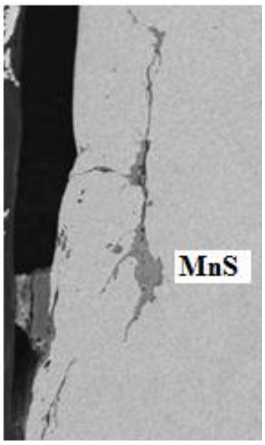

Fig. 3. View of surface damage due to the existence of MnS areas, with (gray color), and crevice corrosion.

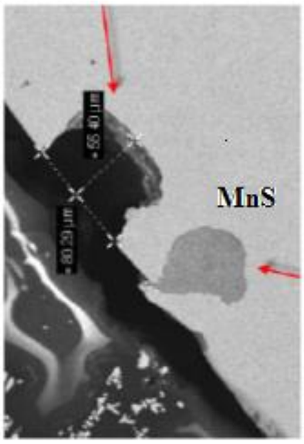

Fig. 4. View of a 90 days corroded specimen where is visible the surface damage (pitting in combination with the presence of MnS inclusions).

Longer exposure up to 90 days enhances phenomenon of close to surface or sub surface MnS dissolution creating a variety of side effects (Fig. 5). Dissolution of MnS segregation sites by Cl- appears to generate local stress concentrations with the possible generation of hydrogen. Due to the position of the MnS sites at depths below up to 500 μm from the surface, the fracture surface exhibits sites, which due to external loads can act as internal stress concentration leading eventually to the formation of cracks.

4. Results of Low Cycle Fatigue Tests and Discussion

Low-cycle-fatigue tests took place on un-corroded (control specimens) and corroded specimens, after exposure to the salt spray chamber for 90 days. For each type of rebar (B400C, B450C and B500B) a free length of 6Φ was selected. Nominal diameter of 6Φ was chosen to simulate steel reinforcing bars in buildings when designing for high ductility class, according to the limits which are set in Eurocode 8 for seismic design of stirrups in reinforced concrete structures. The tests took place under strain control, and were executed by considering two different levels of imposed deformation, respectively equal to ± 2.5 % and ± 4.0 % with sinusoidal cycling frequency 2.0 Hz. The low cycle fatigue tests were performed on the servo-hydraulic MTS 250 kN machine. The number of cycles to failure, the dissipated energy, and the maximum tensile and compressive force per fatigue cycle of the steel bars were evaluated.

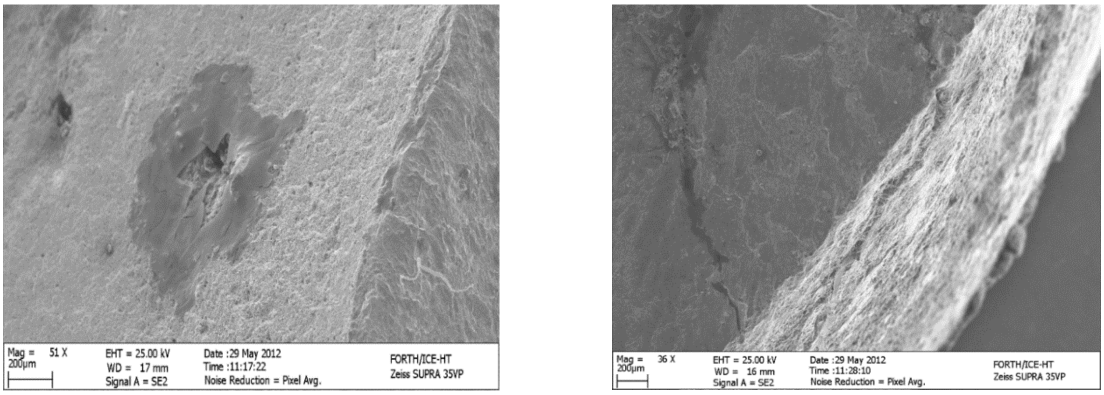

a) b)

Fig. 5. a) Surface failure of 90 days corroded specimen with existence of MnS inclusions and voids. b) Surface failure with crack which was grown in the material structure.

From all the tables in Table 3 is summarized the effect of corrosion on the total dissipated energy density and the total life time of all categories of steel rebars. The observed appreciable reduction may represent a serious problem for the safety of constructions in seismically active areas. As can be seen from the Table 3, the energy storage capacity of the material and the total energy that can be dissipated by the material until failure, is highly dependent on the stain amplitude at which the specimens are subjected. During the seismic erection, the need for a sufficient energy storage capacity of the material is imperative. As expected, the degree of corrosion damage has a significant impact on number of cycles to failure. This shows that as strain levels are increased, corrosion has a smaller impact on the number of cycles to failure, as backed up by the dissipated energy.

In any case, the existence of damage (due to MnS inclusions, voids) inside the structure of steel rebars and especially their development over time of corrosion internally is serious responsible about their failure due to fatigue. It is also important to note that buckling from the first loading cycles creates increased tension on a single side of the rebar. The process is so strong as to produce rapid ductility exhaustion (hardening plateau) and therefore pits within this region (MnS inclusions) will propagate into cracks without any significant ductility signs in their crack path.

Table 3. Low cycle fatigue results for non corroded and corroded specimens in three grades of Φ16 steel bars.

B450C-Φ16 reference				
Sample	Free Length	strain [%]	Cycles to failure	Dissipated energy [MPa]
49	6Φ	±2,5%	35	744.21
50			29	519.77
51			36	756.17
52			33	700.50
60			34	768.04
MEAN VALUE			**33**	**697.74**
53	6Φ	±4,0%	11	439.50
54			11	556.56
55			11	560.37
56			10	558.00
MEAN VALUE			**11**	**528.61**

B450C-Φ16 90 days corroded					
Sample	Free Length	strain [%]	Cycles to failure	Dissipated energy [MPa]	Mass loss [%]
36	6Φ	±2,5%	16	416.06	8.81
40			18	470.93	9.4
23			13	343.23	9.38
MEAN VALUE			**16**	**410.07**	**9.20**
39	6Φ	±4,0%	8	374.1	9.34
34			8	365.8	8.17
30			12	296.2	10.1
26			7	296.2	8.15
MEAN VALUE			**9**	**333.08**	**8.94**

B500B - Φ16 90days corroded					
Sample	Free Length	strain [%]	Cycles to failure	Dissipated energy [MPa]	Mass loss [%]
34	6Φ	±2,5%	19	475,8	8,9
28			18	480,9	9,65
31			17	438,7	9,95
MEAN VALUE			**18**	**465,13**	**9,5**
29	6Φ	±4,0%	7	347,4	8,48
33			6	296,1	9,71
35			7	347,1	8,72
39			7	317,5	8,65
MEAN VALUE			**6**	**327,02**	**8,89**

B400C - Φ16 90days corroded					
Sample	Free Length	strain [%]	Cycles to failure	Dissipated energy [MPa]	Mass loss [%]
37	6Φ	±2,5%	13	337,21	9,57
40			15	360,62	9,6
24			25	560,5	8,4
MEAN VALUE			**17**	**419,4**	**9,19**
35	6Φ	±4,0%	7	311,3	8,79
31			7	318,4	9,65
28			7	327,4	9,2
MEAN VALUE			**7**	**319,03**	**9,21**

B500B - Φ16 reference				
Sample	Free Length	strain [%]	Cycles to failure	Dissipated energy [MPa]
47	6Φ	±2,5%	35	761,39
49			31	732,2
60			29	655,1
61			30	727,62
MEAN VALUE			**31**	**719,08**
52	6Φ	±4,0%	11	325,97
54			11	435,93
62			10	387,32
63			11	411,74
MEAN VALUE			**10**	**390,24**

B400C - Φ16 reference				
Sample	Free Length	strain [%]	Cycles to failure	Dissipated energy [MPa]
49	6Φ	±2,5%	22	470,5
52			24	505,6
60			25	558,15
61			27	610,54
MEAN VALUE			**24**	**523,34**
53	6Φ	±4,0%	10	515,5
54			8	503,4
55			11	510,5
63			11	371,65
MEAN VALUE				**484,45**

After studying the results of tests, all the EDX and SEM which were presented, lead to the following views:

1. Corrosion causes internal pitting of MnS particles, which follow their original particle congregation prior to pitting. The pitting has significant surface dimension and the damage extends in depth.

2. Upon loading these locations act as internal stress concentration leading eventually to the formation of cracks. However due to their proximity they force a multiple cracking phenomenon. As such crack coalescence will become critical with the number of loading cycles leading to fast crack growth. The direction of the crack appears to tend to expand towards the surface.

3. This rapid expansion of the crack produces brittle ridge-like fracture surface- negating any remaining ductility that had been left in the material. Yet pits which are not congregate in a similar way (single MnS particles) will produce some sort of quasi brittle LCF surface.

4. It is also important to note that from the first loading cycles buckling creates increased tension on a single side of the rebar. The process is so strong as to produce rapid ductility exhaustion (hardening plateau) and therefore pits within this region will propagate into cracks without any significant ductility signs in their crack path.

5. It is our conclusion that the fracture surface of the rebar is a mixture of more than 2 failure mechanisms which due to their nature produced in nature a mainly brittle type failure with limited signs of traditional LCF. It is also imperative to acknowledge that due to buckling

and buckling reversal the material's ductility especially at 4 % is particularly limited and it might be exhausted prior to the formation of the cracks. Concrete evidence of the sequence of events within such limited cycle duration are impossible to be extracted.

6. From a Fracture Mechanics perspective the case postulates void growth analysis according to Dugdale's theory.

The assessment of structure performance in older buildings which is based only on mathematical models (displacement–pushover method) might lead to unreliable and inappropriate decisions when the degradation of the strength and ductility properties of materials due to corrosion is not taken into consideration beforehand.

5. Conclusions

The mechanical behavior of high performance steel rebars B400c, B450c and B500b (with existence of martensite in the outer zone) under seismic loads in environment of corrosion needs to be studied further. A basic reason for the above view is the existence of MnS inclusions in some regions where MnS acts as internal stress concentration leading eventually to the formation of cracks. However due to their proximity they force to a multiple cracking phenomenon. Moreover, corrosive environment causes strong outer pits and also increasing the areas of MnS, this combination leads to unpredictable consequences for the structural integrity of the steel reinforcement over time.

References

[1] G.M. Sheng, S.H. Gong // *Acta Metallurgica Sinica (English Letters)* **10** (1997) 51.
[2] Y.H. Chai // *Earthquake Engineering and Structural Dynamics* **34** (2005) 83.
[3] S.Y.M. Ma, V.V. Bertero, E.P. Popov, *Experimental and Analytical Studies on the Hysteretic Behavior of Reinforced Concrete Rectangular and T-Beams*. Earthquake Engineering Research Report (University of California, Berkeley, USA, 1976), Vol. 76(2).
[4] T. Yoshaki, In: *Proceedings of Academical Lectures of JAS* (Tokyo, 1983), p. 606.
[5] H. Shigeru, *Retrofitting of Reinforced Concrete Moment Resisting Frame*, Research report supervised by R. Park and H. Tanaka (1995).
[6] G.G. Clementa, *Testing of selected metallic reinforcing bars of extending the service life of future concrete bridges*. Fin. report (Virginia Transport, Charlot, VA, Research Council, VTRC 03-A7, 2002).
[7] H. Krawinkler // *Earthquake Spectra* **3** (1987) 27.
[8] I. Kasiraj, J.T.P. Yao //*Journal of the Structural Division (ASCE)* **95** (1969) 1673.
[9] G. Kodzhaspirov (Kodjaspirov), In: *Proceedings of the 5th Europian Conference on advanced Materials, Processes and Applications* (Maastrict, Netherland, 1997), Vol. 1, p. 673.
[10] Ch. Apostolopoulos, G. Diamantogiannis, Alk. Apostolopoulos // *Journal of Materials in Civil Engineering (ASCE)* **28(2)** (2016).
[11] J.E. Castle, R. Ke // *Corrosion Science* **30**(1990) 409.
[12] M.A. Baker,J.E. Castle // *Corrosion Science* **34 (4)**(1993) 667.
[13] B. Lin, R. Hu, Ch. Ye, Y. Li, Ch. Lin // *Electrochimica Acta Journal* **55**(2010) 6542.
[14] Project Rusteel, *"Effects of Corrosion on Low-Cycle Fatigue (Seismic) Behavior of High Strength Steel Reinforcing Bars" RFS-PR-8017, 2009-2012*.